Supporting Information

Highly efficient sulfur cathode built by biomass hierarchical porous carbon for aqueous Cu-S battery

Xue Han [a,1], Jiaxi Xu [a,1], Haoxiang Yu [a,], Junwei Zhang [a], Yiwen Liu [a], Junyi Wang [a], Zhouxiang Wu [a], Zhongjie Shu [b,*], Lei Yan [a], Liyuan Zhang [a], Jie Shu [a,*]*

[a] *School of Materials Science and Chemical Engineering, Ningbo University, Ningbo, Zhejiang, 315211, China*

[b] *Sinochem Lantian Fluoro Materials Co., Ltd., Shaoxing, Zhejiang 312369, China*

[1] These authors contributed equally to this work

* Corresponding author: Jie Shu

E-mail: shujie@nbu.edu.cn

* Corresponding author: Haoxiang Yu

E-mail: yuhaoxiang@nbu.edu.cn

* Corresponding author: Zhongjie Shu

E-mail: shuzhongjie@sinochem.com

Experimental

Preparation of NHPC

Firstly, the collected pomegranate peel was cut into pieces and washed by deionized water to make it no impurities on the surface, and then dried at 80 °C for 24 h. Afterward, the dried pomegranate peel was pre-carbonized at the temperature of 350 °C for 2 h under Ar atmosphere with 5 °C min^{-1} heating rate in a tubular furnace. Then, to prepare highly porous pomegranate peel derived biochar, KOH and carbon formed by pyrolysis were added into the 10 mL deionized water in 4:1 mass proportion, stirring at 60 °C until dried. As the activating reagent for the reaction, KOH reacts with carbon in the redox reactions and corrodes the carbon framework. The gaseous H_2O and CO_2 produced by these activation reactions facilitate the increase of carbon porosity to improve the affinity with sulfur. After that, the obtained mixture was held in an 800 °C tubular furnace which was heated from room temperature with a heating rate of 4 °C min^{-1}. Subsequently, we washed it with deionized water several times until pH=7 and dried it at 60 °C.

Synthesis of S@NHPC

The mixture of activated biochar and sulfur in the weight ratio of 3:7 was ground 30 min in an agate mortar sufficiently. Then, they were transferred to a hydrothermal reactor and maintained at 155 °C for 10 h.

Materials characterizations

The crystal structure of material was collected by X-ray diffraction (XRD, Bruker AXS D8 Advance) with Cu-Kα radiation (λ=1.5406 Å). The surface and

morphology of the material was obtained by scanning electron microscope (SEM, Sirion 200, FEI Co., USA) and transmission electron microscope (TEM, JEM-7650, JEOL Inc., Japan). X-ray photoelectron spectroscopy was conducted on an XSAM800 Ultra spectrometer. Raman spectra of the carbon materials was performed with a laser Raman spectrometer (LabRam-HR, HORIBA Jobin Yvon Co., France). Brunauer-Emmett-Teller (BET) surface area was measured by ASAP 2460 instrument by nitrogen adsorption at 77 K. TGA was performed on a TG/DTA7300 (Seiko In.).

Electrochemical measurements

For preparing working electrode, the slurry was made by the mixture of S@NHPC, acetylene black, and PTFE in the weight ratio of 8:1:1. The slurry was uniformly smeared onto carbon paper current collector (1 cm^2) and dried at 60 °C for 12 h to fabricate the working electrode. In S@NHPC, the weight ratio of the activated biochar and sulfur is 3:7, and the TG confirms that there is ~66% of sulfur in S@NHPC. In the working electrode, the mass loading of sulfur was ~1.2 mg cm^{-2}.

The electrochemical properties of samples were evaluated in coin cell, which consisted of working electrode, counter electrode (copper), separator (Whatman), and 0.5 mol L^{-1} $CuSO_4$ electrolyte (~1 mL). The CV curves were conducted on a Bio-Logic VSP electrochemical workstation. Galvanostatic charge/discharge, cycling performance, and rate performance were investigated by a LANHE battery tester (LANHE CT2001C).

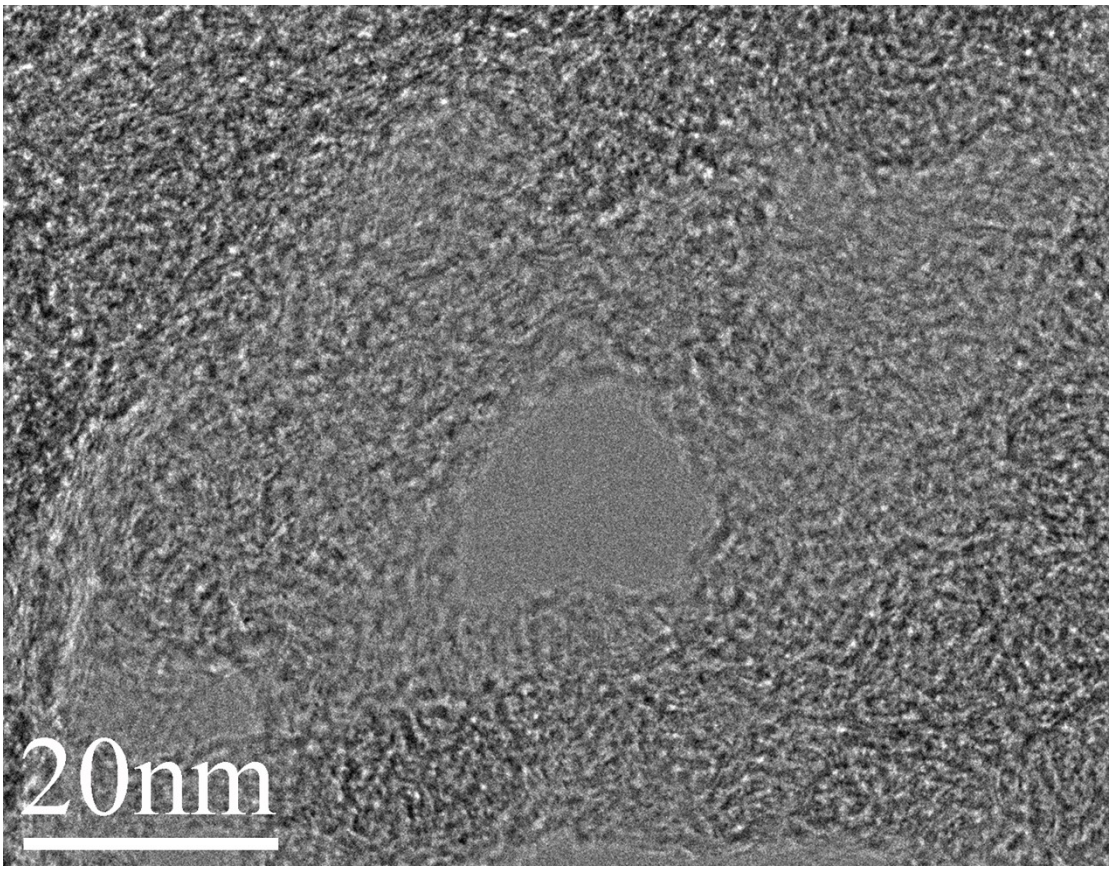

Fig. S1. HRTEM image of NHPC

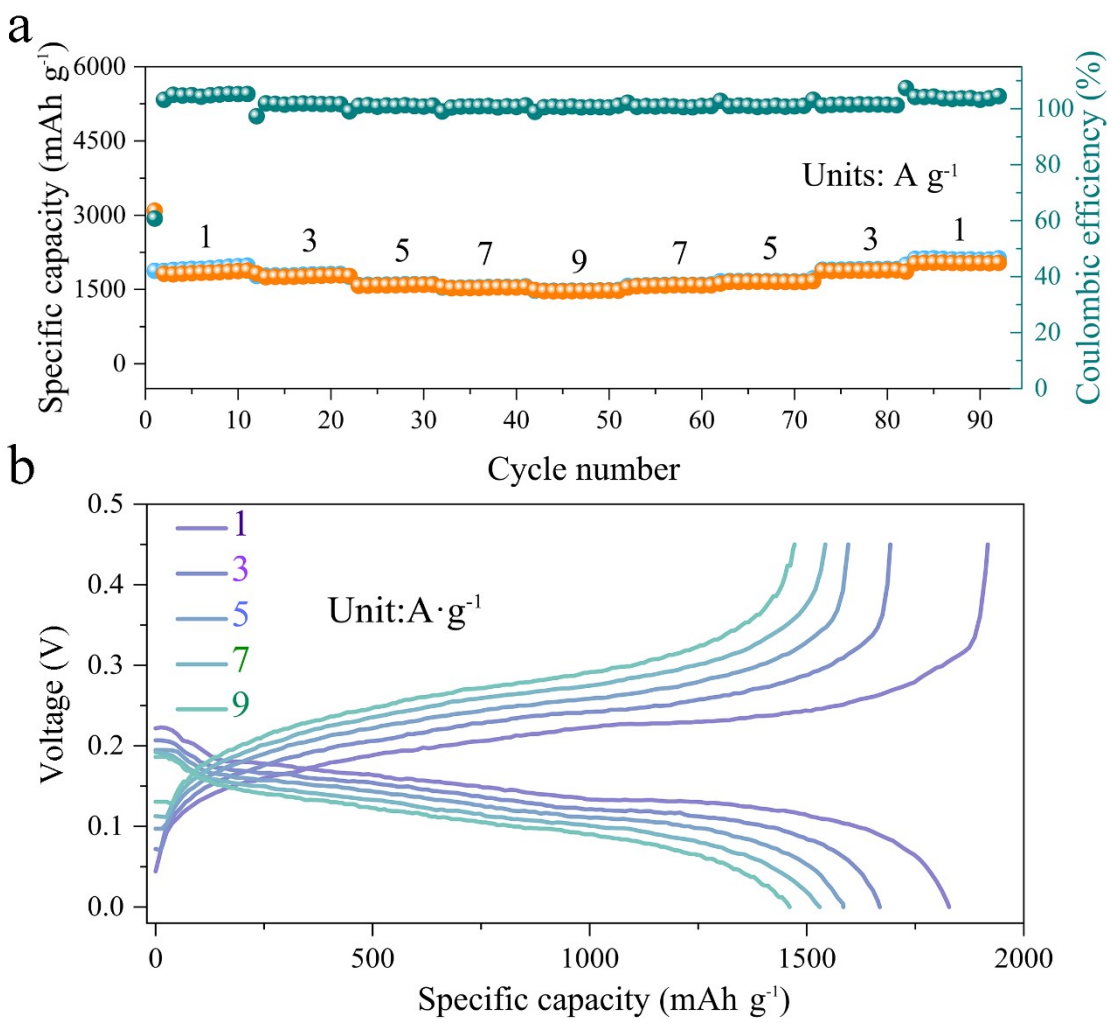

Fig. S2. (a-b) Rate performance based on different current densities (from 1 to 9 A g^{-1})

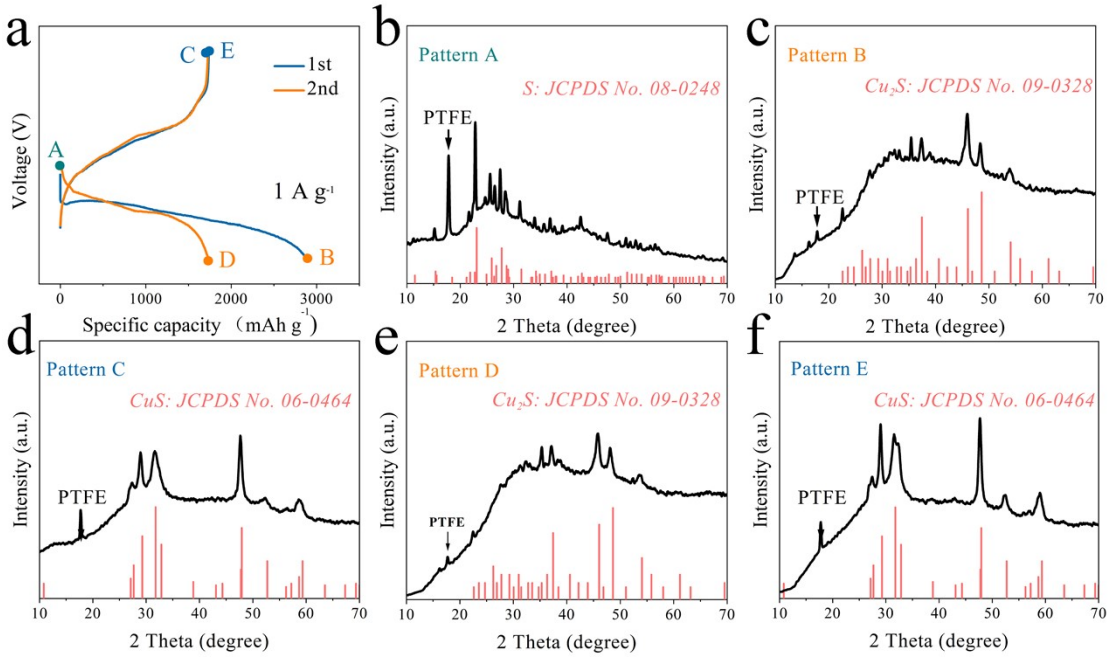

Fig. S3. XRD patterns of S@NHPC electrodes. a) Galvanostatic charge/discharge profiles at a current rate of 1 A g^{-1}; b) XRD pattern of the pristine S@NHPC electrodes; c) XRD pattern of the fully pre-discharged S@NHPC electrodes; d) XRD pattern of the fully pre-charged S@NHPC electrodes; e) XRD pattern of the fully discharged S@NHPC electrodes; f) XRD pattern of the fully charged S@NHPC electrodes

Table S1. The specific capacity of reported S-based battery.

Battery	Cathode	Current density ($A\ g^{-1}$)	Specific capacity ($mAh\ g^{-1}$)	Ref.
	pure sulfur (copper wire-graphene/polyimide/LLZO trilaminar membrane)	0.1	1402	S1
Li-S	S–G	0.2088	1261	S2
	fibrous graphene-sulfur	0.3	1160	S3
	the sulfur/3D graphene composite	3.35	500	S4
	S@Fe-PANi	0.1	720	S5
Zn-S	LF-PLSD	0.5	488	S6
	LF-PLSD	1	300	S6
K-S	CMK-3/sulfur	0.01	606	S7
	CMK-3/sulfur	0.05	512.7	S7
Fe-S	S/AC-40	0.2	950	S8
	S/AC-40	0.5	890	S8
	S/AC-40	0.8	831	S8
	S/AC-40	1	796	S8
	S/AC-40	1.5	686	S8
Al-S	S@HKUST-1-C	0.5	689	S9

	S@HPCK	1	530	S10
	CS90	0.2	542	S11
Na-S	N,S-HPC	0.23	400	S12
	N,S-HPC	4.6	128	S13

Table S2. The capacity retention of reported S-based battery.

Battery	Cathode	Cycle number	Capacity retention (%)	Current density	Ref.
Li-S	3D-VCNs	300	80.3	0.837 A g^{-1}	S14
	S-rGO	450	87	1 C	S14
	S@MLC-2	500	60	0.5 C	S15
	S@HCSs	1200	43.6	0.5 C	S16
Al-S	S@HKUST-1-C	50	52.1	1 A g^{-1}	S9
	S@HKUST-1-C	500	41.7	1 A g^{-1}	S9
Mg-S	MgS_8@Graphene-CNT	50	83.3	0.083 A g^{-1}	S17
	S@CNT	100	81.7	0.5 A g^{-1}	S18
	ZIF-C-S	200	66.7	1 C	S19
Na-S	CSB@TiO_2	400	63.1	0.5 A g^{-1}	S20
	S@iMCHS	200	88.8	0.1 A g^{-1}	S13
K-S	Sulfurized carbonized polyacrylonitrile	100	95	1.675 A g^{-1}	S21
	Confined and covalent sulfur	300	86.3	0.6 A g^{-1}	S22

	CNTs/S	60	95	0.3 A g^{-1}	S23
Pb-S	CNTs/S	140	88	0.5 A g^{-1}	S24
	CNTs/S	400	71.4	0.5 A g^{-1}	S24

References

S1 X. Liu, Y. Li, X. Xu, L. Zhou, L.Q. Mai, Rechargeable metal (Li, Na, Mg, Al)-sulfur batteries: Materials and advances, *J. Energy Chem.*, 2021, **61**, 104-134.

S2 B. Li, S. Li, J. Liu, B. Wang, S. Yang, Vertically aligned sulfur-graphene nanowalls on substrates for ultrafast lithium-sulfur batteries, *Nano Lett.*, 2015, **15**, 3073-3079.

S3 G. Zhou, L.C. Yin, D.W. Wang, L. Li, S. Pei, I.R. Gentle, F. Li, H.M. Cheng, Fibrous hybrid of graphene and sulfur nanocrystals for high-performance lithium-sulfur batteries, *ACS Nano*, 2013, **7**, 5367-5375.

S4 C. Xu, Y. Wu, X. Zhao, X. Wang, G. Du, J. Zhang, J. Tu, Sulfur/three-dimensional graphene composite for high performance lithium-sulfur batteries, *J. Power Sources*, 2015, **275**, 22-25.

S5 H. Zhang, Z.T. Shang, G. Luo, S.H. Jiao, R.G. Cao, Q.W. Chen, K. Lu, Redox catalysis promoted activation of sulfur redox chemistry for energy-dense flexible solid-state Zn-S battery, *ACS Nano*, 2022, **16**, 7344-7351.

S6 Y.W. Zhao, D.H. Wang, X.L. Li, Q. Yang, Y. Guo, F.N. Mo, Q. Li, C.X. Peng, H.F. Li, C.Y. Zhi, Initiating a reversible aqueous Zn/sulfur battery through a "Liquid Film", *Adv. Mater.*, 2020, **32**, 2003070.

S7 L. Wang, J. Bao, Q. Liu, C.F. Sun, Concentrated electrolytes unlock the full energy potential of potassium-sulfur battery chemistry, *Energy Storage Mater.*, 2019, **18**, 470-475.

S8 X.Y. Wu, A. Markir, Y.K. Xu, E.C. Hu, K.T. Dai, C. Zhang, W. Shin, D.P.

Leonard, K. Kim, X.L. Ji, Rechargeable iron-sulfur battery without polysulfide shuttling, *Adv. Energy Mater.*, 2019, **9**, 1902422.

S9 Y. Guo, H. Jin, Z. Qi, Z. Hu, H. Ji, L.J. Wan, Carbonized-MOF as a sulfur host for aluminum-sulfur batteries with enhanced capacity and cycling life, *Adv. Funct. Mater.*, 2019, **29**, 1807676.

S10 D. Zhang, X. Zhang, B.Y. Wang, S.M. He, S.Q. Liu, M.X. Tang, H.J. Yu, Highly reversible aluminium-sulfur batteries obtained through effective sulfur confinement with hierarchical porous carbon, *J. Mater. Chem. A*, 2021, **9**, 8966-8974.

S11 A. Ghosh, S. Shukla, M. Monisha, A. Kumar, B. Lochab, S. Mitra, Sulfur copolymer: A new cathode structure for room-temperature sodium-sulfur batteries, *ACS Energy Lett.*, 2017, **2**, 2478-2485.

S12 Z. Qiang, Y.M. Chen, Y. Xia, W. Liang, Y. Zhu, B.D. Vogt, Ultra-long cycle life, low-cost room temperature sodium-sulfur batteries enabled by highly doped (N,S) nanoporous carbons, *Nano Energy*, 2017, **32**, 59-66.

S13 Y.Z. Wang, D. Zhou, V. Palomares, D. Shanmukaraj, B. Sun, X. Tang, C.S. Wang, M. Armand, T. Rojo, G.X. Wang, Revitalising sodium-sulfur batteries for non-high-temperature operation: A crucial review, *Energy Environ. Sci.*, 2020, **13**, 3848-3879.

S14 T. Li, X. Bai, U. Gulzar, Y.J. Bai, C. Capiglia, W. Deng, X.F. Zhou, Z.P. Liu, Z.F. Feng, R.P. Zaccaria, A comprehensive understanding of lithium-sulfur battery technology, *Adv. Funct. Mater.*, 2019, **29**, 1901730.

S15 B. He, W.C. Li, C. Yang, S.Q. Wang, A.H. Lu, Incorporating sulfur inside the pores of carbons for advanced lithium-sulfur batteries: An electrolysis approach, *ACS Nano*, 2016, **10**, 1633-1639.

S16 A. Chen, Y. Yu, H. Lv, Y. Wang, S. Shen, Y. Hu, B. Li, Y. Zhang, J. Zhang, Thin-walled, mesoporous and nitrogen-doped hollow carbon spheres using ionic liquids as precursors, *J. Mater. Chem. A*, 2013, **1**, 1045-1047.

S17 Y. Xu, G. Zhou, S. Zhao, W. Li, F. Shi, J. Li, J. Feng, Y. Zhao, Y. Wu, J. Guo, Improving a Mg/S battery with YCl_3 additive and magnesium polysulfide, *Adv. Sci.*, 2019, **6**, 1800981.

S18 A. Du, Z.H. Zhang, H.T. Qu, Z.L. Cui, L.X. Qiao, L.L. Wang, J.C. Chai, T. Lu, S.M. Dong, T.T. Dong, H.M. Xu, X.H. Zhou, G.L. Cui, An efficient organic magnesium borate based electrolyte with non-nucleophilic characteristic for magnesium sulfur battery, *Energy Environ. Sci.*, 2017, **10**, 2616-2625.

S19 Y. Lu, C. Wang, Q. Liu, X.Y. Li, X.Y. Zhao, Z.P. Guo, Progress and perspective on rechargeable magnesium-sulfur batteries, *Small Methods*, 2021, **5**, 2001303.

S20 D. Ma, Y. Li, J. Yang, H. Mi, S. Luo, L. Deng, C. Yan, M. Rauf, P. Zhang, X. Sun, X. Ren, J. Li, H. Zhang, New strategy for polysulfide protection based on atomic layer deposition of TiO_2 onto ferroelectric-encapsulated cathode: Toward ultrastable free-standing room temperature sodium–sulfur batteries, *Adv. Funct. Mater.*, 2018, **28**, 1705537.

S21 J.Y. Hwang, H.M. Kim, Y.K. Sun, High performance potassium-sulfur batteries based on a sulfurized polyacrylonitrile cathode and polyacrylic acid binder, *J.*

Mater. Chem. A, 2018, **6**, 14587-14593.

S22 J. Ding, H. Zhang, W.J. Fan, C. Zhong, W.B. Hu, D. Mitlin, Review of emerging potassium-sulfur batteries, *Adv. Mater.*, 2020, **32**, 1908007.

S23 C.W. Xu, Z.W. Yang, H.H. Yan, J. Lia, H.X. Yu, L.Y. Zhang, J. Shu, Synergistic dual conversion reactions assisting Pb-S electrochemistry for energy storage, *Proc. Natl. Acad. Sci. U. S. A.*, 2022, **119**, e2118675119.